

Synthesis, characterization, and utilization of a lignin-based adsorbent for effective removal of azo dye from aqueous solution

Xianzhi Meng^{†}, Brent Scheidemantle^{‡,§}, Mi Li[†], Yunyan Wang[†], Xianhui Zhao[⊥], Miguel Toro-González[#], Priyanka Singh^{‡,§}, Yunqiao Pu^{//}, Charles E. Wyman^{‡,§}, Soydan Ozcan^{∇,Ω}, Charles M. Cai^{‡,§}, Arthur J. Ragauskas^{†, //, Φ*}*

[†] Department of Chemical & Biomolecular Engineering, University of Tennessee Knoxville, Knoxville, TN 37996, USA

[‡] Center of Environmental and Research Technology (CE-CERT), University of California, Riverside, CA 92507, USA

[§] Department of Chemical and Environmental Engineering, Bourns College of Engineering, University of California, Riverside, CA 92521, USA

[⊥] Chemical Sciences Division, Oak Ridge National Laboratory, Oak Ridge, TN 37831, USA

[#] Isotope and Fuel Cycle Technology Division, Oak Ridge National Laboratory, Oak Ridge, TN 37831, USA

^{//} Biosciences Division, Oak Ridge National Laboratory, Oak Ridge, TN 37831, USA

[∇] Department of Mechanical, Aerospace, Biomedical Engineering, University of Tennessee, Knoxville, TN 37996, USA

^Ω Manufacturing Demonstration Facility, Energy and Transportation Science Division, Oak Ridge National Laboratory, Knoxville, TN 37932 USA

^Φ Department of Forestry, Wildlife, and Fisheries; Center for Renewable Carbon, The University of Tennessee Knoxville, Institute of Agriculture, Knoxville, TN 37996, USA

ABSTRACT

How to effectively remove toxic dyes from the industrial wastewater using green low-cost lignocellulose-based adsorbent such as lignin has become a topic of great interest but remains quite challenging. In this study, Co-solvent Enhanced Lignocellulosic Fractionation (CELf) pretreatment and Mannich reaction were combined to generate aminated CELf lignin which is subsequently applied for removal of Methylene Blue (MB) and Direct Blue (DB) 1 dye from aqueous solution. ^{31}P NMR was used to track degree of amination, and an orthogonal design was applied to determine the relationship between extent of amination and reaction parameters. The physicochemical, morphological, and thermal properties of the aminated CELf lignin were characterized to confirm the successful grafting of DETA onto the lignin. The aminated CELf lignin proved to be an effective azo dye-adsorbent, demonstrating considerably enhanced dye decolorization, especially toward DB 1 dye (>90%). It had a maximum adsorption capacity of DB 1 dye of 502.7 mg/g, and the kinetic study suggested the adsorption process conformed to a pseudo-second-order kinetic model. The isotherm results also showed that the modified lignin-based adsorbent exhibited monolayer adsorption. The adsorbent properties were mainly attributed to the incorporated amine functionalities as well as the increased specific surface area of the aminated CELf lignin.

Keywords:

Lignin Amination, Co-Solvent Enhanced Lignocellulosic Fractionation, Lignin Valorization, Mannich reaction, dye-adsorbent

INTRODUCTION

The demand for clean water is likely to increase driven by the rapid urbanization, expanding industrial activities, energy generation, and water pollution. Due to the limited fresh water resources on earth, this demand should be addressed by developing promising water purification techniques. The presence of organic dyes in industrial wastewater could cause some serious environmental concerns due to their poor biodegradability and toxicity to the exposed plants, living organisms, and even human being. As a result, those toxic dyes should be removed from the wastewater as much as possible before being discharged to land or water sources in an environmentally friendly manner.¹ The textile industry consumes organic dyes which represent 60% of the world's dye consumption, and it was reported that 10-25% of water-soluble dyes are lost during the dyeing process and 2-20% of dyes are released as effluent into the water system after the dyeing process.² Azo dyes are known as dyes containing $-N=N-$ groups, representing 60-70% of commercially available dyes in the world.³ They are extensively used in the textile industry, and become part of the textile effluents. Therefore, how to cost-effectively remove these toxic azo dyes from the industrial wastewater has become a topic of great interest.

Adsorption is considered as an alternative method to the traditional combination of chemical and biological processes for the removal of dyes from aqueous solutions.⁴⁻⁵ Dye adsorption by various adsorbents is considered to occur primarily via π interaction, hydrogen bonding, and electrostatic interactions. Several organic and inorganic materials including zeolite,^{2,6} lignocellulosic substrate,⁷⁻⁸ activated carbon,⁹ graphite,¹⁰ and graphene oxide have been all tested

and shown to have different adsorption activities toward organic dyes in wastewater.¹¹⁻¹² Some of these adsorbents have a rather high dye removal efficiency, however, low-cost renewable green bio-adsorbents are still rare for this field of application and further studies are urgently required.¹³

The biorefinery concept has received considerable attention in the last decade due to advances in biotechnology and genetic engineering, offering a renewable and sustainable alternative to the production of common petrochemicals.¹⁴ Abundant lignocellulosic biomass is a second-generation non-food feedstock that, when used by future biorefineries, has the potential to significantly offset the carbon footprint of the traditional refining.¹⁵ As one of the most important renewable fractions found in biomass, lignin is still significantly underutilized in the current biorefinery industries, which has mainly focused on transforming biomass carbohydrates to liquid fuels.¹⁶ It is anticipated that with the growing demand of biomass for production of fuels, the production of lignin would also substantially increase, potentially serving as a versatile platform for the production of biopolymers and renewable high-performance materials. The Renewable Fuel Standard (RFS) established in 2005 and further expanded in 2007 by the Energy Independence and Security Act (EISA) aims to ascend to 36 billion gallons of renewable fuel in 2022. Assuming a yield of 335 liters per dry Mg of biomass, 223 million Mg of biomass will be used annually, producing about 62 million Mg of lignin.¹⁷ To avoid using lignin as a low-grade boiler fuel, new thermal and chemical processes are needed to generate value-added products from lignin.

Lignin macromolecule contains various amounts of functional groups including carbonyl, methoxy, carboxyl, and hydroxyl groups, which offers promising opportunities to take advantage of its versatile functionality for multiple applications.¹⁸ Without any further chemical treatments, lignin could be directly incorporated into a polymeric matrix to be served as an antioxidant,¹⁹ a flame retardant,²⁰ dye adsorbent,²¹⁻²² and a UV stabilizer.²³ Given the diversity of lignin, variability in performance as a functionalized polymer is expected to depend on the plant sources, lignin isolation methods, and physicochemical structures of lignin. Thus, chemical modifications of lignin to improve its valorization have attracted growing attentions.²⁴⁻²⁵ Lignin amination refers to a process that introduces an amine group into the lignin structure. One of the bases of lignin amination is the Mannich reaction which refers to the reaction between lignin and amine in the presence of formaldehyde. The obtained aminated lignin, has properties that make it ideal for use in several applications, including surfactants,²⁶ dispersants,²⁷ heavy metal adsorbents,²⁸ and asphalt emulsifiers.²⁹⁻³⁰ Due to its aromatic/phenolic nature and cationic side chain, aminated lignin could have great potential as a low-cost bio-adsorbent for the removal of organic dyes especially azo dyes that are typically anionic in charge in wastewater.

Here, we used a Co-solvent Enhanced Lignocellulosic Fractionation (CELf) method as a highly effective lignin-first pretreatment approach capable of extracting highly pure technical-grade lignin from corn stover. CELf applies aqueous mixture of tetrahydrofuran (THF) and dilute acid to greatly enhance the fractionation of lignin, hemicellulose, and cellulose fractions in biomass while promoting lignin fragmentation by limiting certain lignin condensation reactions

typically suffered at high reaction severities. The obtained CELF lignin is depolymerized, containing lower aryl ether linkages and higher phenolic hydroxyl groups than typical native milled wood lignin (MWL), cellulolytic enzyme lignin (CEL), or Kraft lignin, which favors the subsequent amination process.³¹⁻³² The isolated CELF lignin was then aminated by diethylenetriamine (DETA) in the presence of formaldehyde under acid conditions via the Mannich reaction. An orthogonal array system was also applied to test the optimal conditions for the Mannich reaction. The obtained final aminated lignin was thoroughly characterized by various analytical techniques including Fourier-transform Infrared Spectroscopy (FTIR), Nuclear Magnetic Resonance spectroscopy (NMR), Scanning Electron Microscopy (SEM), Thermal Gravimetric Analysis (TGA), and Brunauer-Emmett-Teller (BET) surface area analysis. Finally, the performance of the obtained aminated CELF lignin as a bio-renewable adsorbent for the removal of methylene blue and direct blue dyes was evaluated and compared to other reported adsorbents from literature. The combinatorial process takes advantage of the selectivity of the Mannich chemistry and the unique versatile functionality of CELF lignin such as low ether linkages and high phenolic OH content. It is fully expected that this study will provide a baseline for future studies to synthesis renewable lignin-based dye adsorbent in advanced wastewater treatment systems.

RESULTS AND DISCUSSION

Synthesis and characterization of adsorbents. Orthogonal experiments. Systematic experimental designs such as response surface methodology and orthogonal arrays are widely

used to obtain the optimal response.³³⁻³⁴ An orthogonal experiment design (L16, 5⁴) including five factors (A: temperature, B: time, C: amine content, D: formaldehyde content, and E: acetic acid content) at four different levels were first applied to determine the optimal Mannich reaction conditions. The Mannich reaction can only occur between a high electron density carbon and an immonium ion formed from formaldehyde and an amine, thus the amine groups are expected to be introduced only at the *ortho* or *para* position of a phenolic hydroxyl group, converting H or G types of free phenolic hydroxyl group (or both) to C₅ substituted hydroxyl groups (Fig. 1).³⁵ This provides a unique opportunity to determine the extent of lignin amination by tracking the content of free H and G phenolic hydroxyl groups. Quantitative ³¹P NMR technique was used to track the content of free H and G phenolic hydroxyl groups, aiming to assess the extent of lignin amination. Table 1 shows the conversion of H and G types of free phenolic hydroxyl for each experiment of the designed orthogonal array. As indicated by the Table 1, the effect of each experiment parameter on the extent of lignin amination increases in this order: acetic acid content (E) < reaction time (B) < DETA content (C) < formaldehyde content (D) < reaction temperature (A) according to the extremum of each factor (R value). The reaction temperature was found to be the most important factor, and the extent of amination appears to achieve its maximum at 75 °C. This could be because the Mannich reaction is an endothermic reaction thus it can be promoted by increasing the temperature. A further increase in temperature has been shown to have a negative effect on amination, which could be due to unnecessary formaldehyde and DETA evaporation thus resulting in a decrease of reaction efficiency.³⁶ In conclusion, the

optimal combination parameters of the experiment are 75 °C, 4 h, 4 mmol DETA, 16 mmol formaldehyde, 0.20 mL acetic acid according to the average values of each factor at different levels (K value). A large scale batch reaction was then performed at this optimal condition, and the obtained aminated CELF lignin was subsequently characterized by several state-of-the-art analytical techniques.

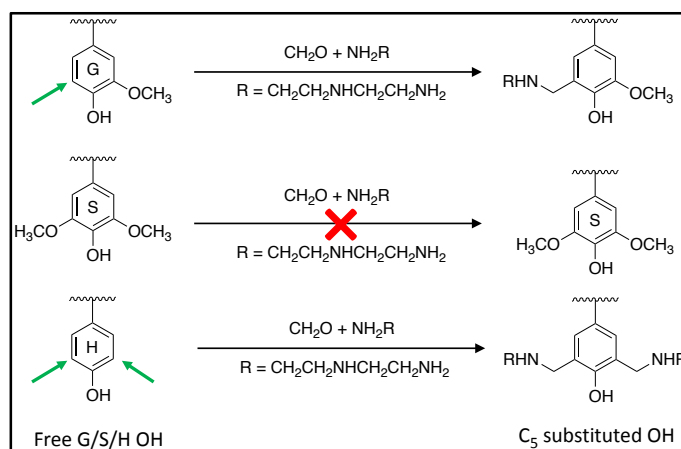


Figure 1. Mannich reaction between phenolic G/S/H lignin and DETA, leading to the formation of phenolic C_5 substituted lignin units.

Table 1. L_{16} (P5)^{L4} orthogonal experiment design of the Mannich reaction between CELF lignin and DETA under acid conditions.*

Experiment**	Temp. (A)	Time (B)	DETA (C)	Formal. (D)	Acid (E)	(G+H) phenolic conversion (%)
1	A1	B1	C1	D1	E1	43.8
2	A1	B2	C2	D2	E2	46.9
3	A1	B3	C3	D3	E3	52.5
4	A1	B4	C4	D4	E4	55.6
5	A2	B1	C2	D3	E4	57.1
6	A2	B2	C1	D4	E3	81.0
7	A2	B3	C4	D1	E2	59.4
8	A2	B4	C3	D2	E1	61.1

9	A3	B1	C3	D4	E2	84.3
10	A3	B2	C4	D3	E1	85.0
11	A3	B3	C1	D2	E4	89.8
12	A3	B4	C2	D1	E3	77.1
13	A4	B1	C4	D2	E3	48.9
14	A4	B2	C3	D1	E4	63.4
15	A4	B3	C2	D4	E1	78.3
16	A4	B4	C1	D3	E2	90.8
K1 ^{***}	49.7	58.5	76.3	60.9	67.0	
K2	64.6	69.1	64.9	61.7	70.3	
K3	84.0	70.0	65.3	71.3	64.9	
K4	70.4	71.1	62.2	74.8	66.4	
R ^{****}	34.3	11.6	13.1	13.9	2.1	
Best quality level	A3	B4	C1	D4	E2	
Optimal combination	75 °C, 4 h, 4 mmol DETA, 16 mmol Formal aldehyde, 0.2 mL acetic acid					

*For each run, 200 mg of lignin was dissolved in 2 mL of dioxane.

**Temperature A1-A4: 45, 60, 75, and 90 °C; Time B1-B4: 1, 2, 3, and 4 h; DETA content C1-C4: 4, 8, 12, and 16 mmol; Formaldehyde content D1-D4: 4, 8, 12, and 16 mmol; Acetic acid content E1-E4: 0.1, 0.2, 0.3, and 0.4 mL.

***K: average value of each factor at different levels;

****R: extremum of each factor.

FTIR analysis. The structural characteristics of the CELF lignin and aminated lignin were analyzed by FTIR as shown in Fig. 2. Results showed that aminated CELF lignin exhibited some basic adsorption peaks of CELF lignin, which indicates that the skeleton structure of lignin remains basically intact during the Mannich reaction. For example, hydroxyl group stretch (3400 cm^{-1}), asymmetrical stretching vibrations of $-\text{CH}_3$ and $-\text{CH}_2-$ (2937 cm^{-1}), and symmetrical stretching vibrations of $-\text{CH}_3$ and $-\text{CH}_2-$ (2844 cm^{-1}) are observed in both lignin samples. Nonetheless, there exist obvious differences between the lignin and aminated lignin samples. For example, the intensity of FTIR peaks associated with the aromatic C–H vibrations including

1603 cm^{-1} and 1512 cm^{-1} from the aminated lignin is significantly lower than that from the original CELF lignin. This is because the Mannich reaction mainly occurred in the aromatic region of lignin.³⁷ In addition, the intensity of FTIR peaks associated with G units including 1267 cm^{-1} (C-O stretch), 1113 cm^{-1} (deformation vibrations of C-H), and 1030 cm^{-1} (aromatic C-H in-plane deformation) and H units such as 1164 cm^{-1} (C-O stretch) is decreased after amination reaction.³⁸ On the other hand, the intensity of syringyl C-O stretch (1325 cm^{-1}) remains relatively strong after Mannich reaction.³⁸ This is because the amine group could be only introduced at C₃ or C₅ position of H lignin and C₅ position of the G units. Finally, a strong peak around 1650 cm^{-1} representing the N-H bending vibrations in amine structure (NH₂) appeared in the aminated lignin, validating the successful addition of the amine.³⁹ The peak of carbonyl group around 1680 cm^{-1} also disappears after Mannich reaction possibly due to the reaction between C=O and primary amines to form imine derivatives known as Schiff bases.⁴⁰

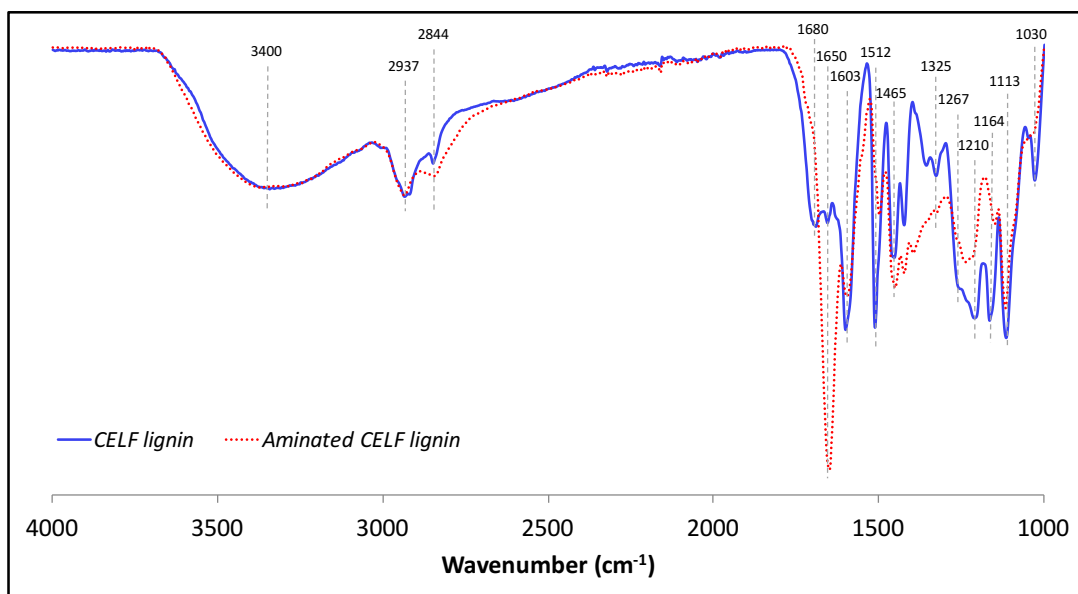


Figure 2. FTIR spectra of corn stover CELF lignin and aminated CELF lignin.

2D HSQC analysis. Two-dimensional HSQC NMR has been comprehensively used in lignin characterization due to its versatility in offering structural insight into the lignin subunits and inter-linkages.⁴¹ The reaction mechanism of Mannich reaction and the chemical structural transformation of CELF lignin during the amination reaction was further characterized by 2D HSQC NMR in this study. As shown in **Fig. 3**, CELF lignin possesses typical structural aromatic patterns of corn stover lignin. Peaks related to S, G, H, p-coumaric acid (*pCA*), ferulic acid (FA), and triclin (T) are all well defined in the aromatic region.⁴² Condensed S and G signals were also found in CELF lignin, which are commonly observed from lignin isolated by cosolvent pretreatment at temperature conditions of 180 °C or higher with acid.⁴³⁻⁴⁵ However, there exist dramatic differences between the original CELF lignin and modified lignin in both the aromatic and aliphatic regions. Specifically, it was found that the cross peaks associated with G and H lignin unit were significantly altered during the Mannich reaction, while the signal of the S lignin units remained relatively stable. In addition, there are two Mannich reactive sites in triclin namely T₆ and T₈ which also disappeared in the aminated lignin due to the reaction of DETA and formaldehyde at these activate aromatic sites. Several intense signals were observed in CELF lignin at δ_C/δ_H 178/9.5-9.6 ppm and δ_C/δ_H 123/7.5 ppm, representing the aldehyde (C _{α}) and furanic C-H (C₃) signal of the 5-substituted furfural derivatives, respectively.⁴¹ It has been reported that these types of furfural derivatives such as 5-hydroxymethylfurfural or 5-(methoxymethyl)furfural which arose from sugar dehydration reactions could be condensed with lignin structure during the acid catalyzed organosolv pretreatments.⁴⁶ These types of structure

were absent after the Mannich reaction possibly due to the reaction between aldehydes and primary amines to form Schiff bases.⁴⁰

In the aliphatic region, lignin interlinkages especially the β -O-4 linkages were dramatically cleaved during the CELF pretreatment process and in fact, these linkages could be only detected at a noise level (data not shown). This is consistent with previous studies that reported CELF pretreatment performed at high severities (180 °C) was capable of achieving near-complete removal of its native β -aryl ether linkages without hydrogen input or further heterogeneous catalytic processing.^{31, 47} This process is expected to generate a substantial amount of phenolic hydroxyl groups that favors the subsequent amination process. Methoxyl group remain as the pronounced functional group in both lignin spectra. Compared to unmodified CELF lignin, a significant amount of new signals appeared in the phenolic lignin side chain of aminated lignin, which was mainly ascribed to the methylene bridge of DETA introduced during the Mannich reaction. Our HSQC analysis also reveals that both the primary and secondary amines are capable of activating the formaldehyde. As shown in Fig. 3, there still exist plenty of secondary amines in our proposed aminated lignin structure, which means as new formaldehyde is activated by these protons, additional reactive phenolic G and H units could be subsequently grafted onto these partially aminated lignins until all the protons on the N atoms are replaced. A schematic diagram of Mannich reaction and the structural transformation of CELF lignin during the amination reaction is shown in Fig. S3. The unmodified and aminated lignin was also subjected to a qualitatively visual Ninhydrin test (Fig. S4). The original CELF lignin had a negative/orange

color indicating the absence of amines, while the change of color in the aminated lignin proved the existence of primary and secondary amine groups.

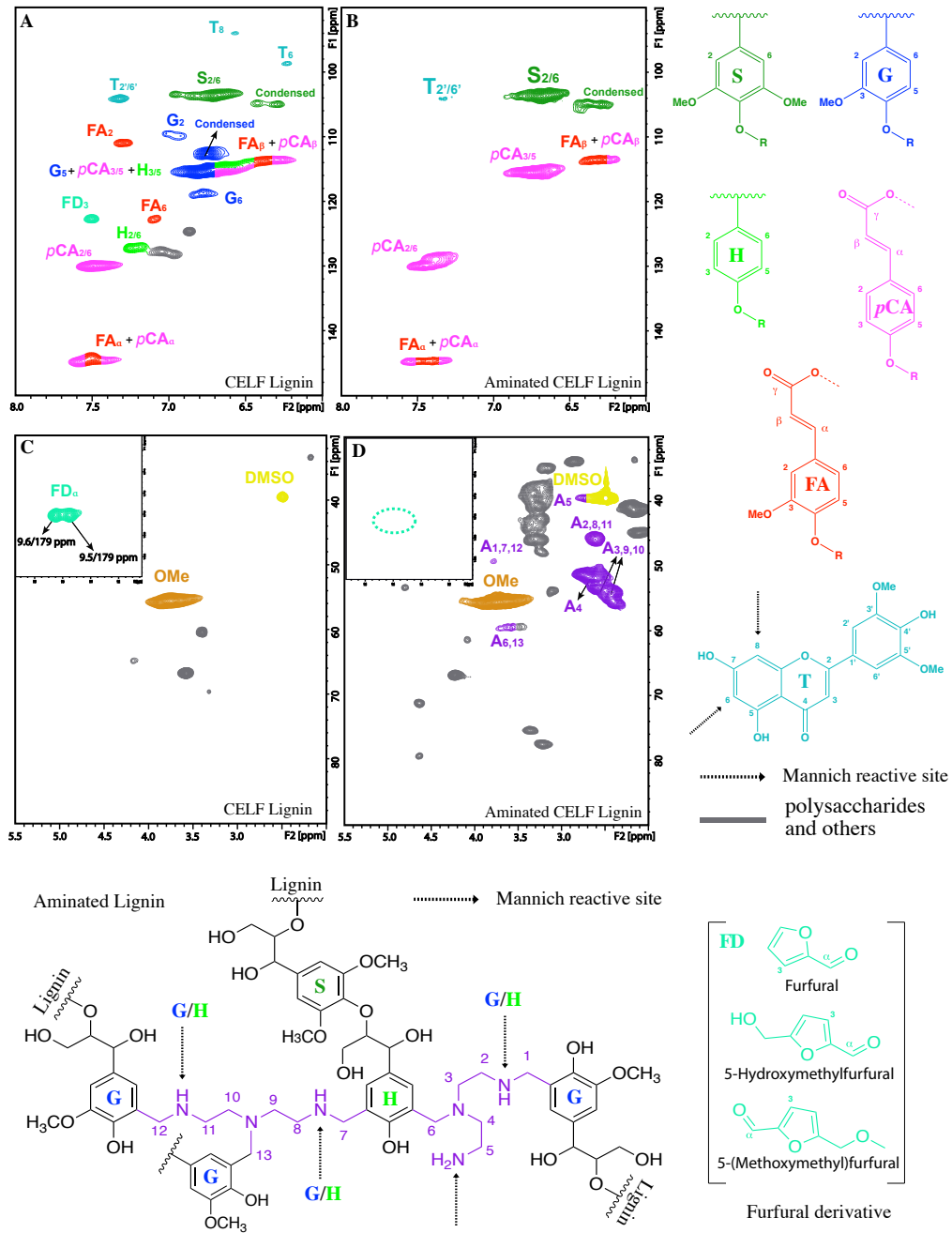


Figure 3. HSQC analysis of the original CELF lignin and its aminated product. (A). CELF lignin aromatic region; (B) aminated lignin aromatic region; (C). CELF lignin aliphatic region; (D). aminated lignin aliphatic region.

³¹P NMR analysis. Quantitative ³¹P NMR technique was further employed to determine different types of hydroxyl groups including aliphatic, phenolic, and carboxylic acid in CELF lignin and aminated lignin and the results are shown in Fig. 4. The phosphitylation reaction of various OHs in lignin structural units with TMDP is shown in Fig. S5. According to a recent study, S hydroxyl group and condensed G hydroxyl groups are not fully baseline resolved and therefore are combined into C₅ substituted hydroxyl groups in this study to avoid any possible overestimation of S and underestimation of G condensed unit.⁴⁸ As compared to the original CELF lignin, a noticeable decrease in phenolic G and H hydroxyl groups was observed in the aminated CELF lignin after Mannich reaction. By contrast, the content of phenolic C₅ substituted hydroxyl groups including the S and condensed G and H units were considerably higher in the modified lignin than that in the original CELF lignin. The ³¹P results also indicated that the reactivity of the reaction sites in G lignin units was higher than that in H lignin, as a result, the proportion of the G unit decreased more obviously than H unit. The slight loss of aliphatic hydroxyl group may result from the possible loss of hydrophilic lignin fragment during the dialysis of aminated lignin.

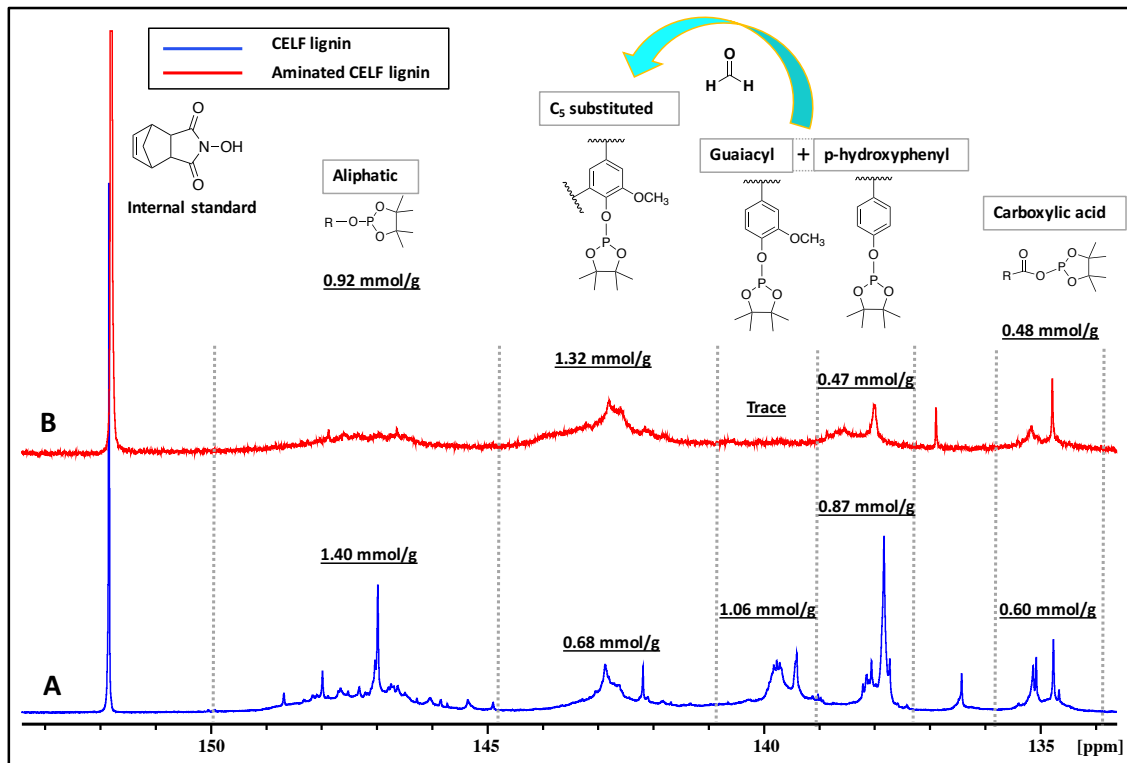


Figure 4. Quantitative ^{31}P NMR spectra of the (A) CELF lignin and (B) aminated lignin.

SEM analysis. The modified lignin sample was obtained by rotatory evaporation, centrifugation followed by extended dialysis and freeze-drying. After repeated vacuum evaporation and centrifugation, the formation of a turbid suspension suggesting the possible presence of aminated lignin nanoparticles. The morphological changes of CELF lignin during Mannich reaction are monitored by SEM and displayed in Fig. 5. The unmodified CELF lignin in the solid state has a much larger particle size compared to the aminated lignin and appears granulated with irregular grains of compact structure. The surface of aminated lignin is much smoother than that of the original lignin. The nano-spheric particles also aggregated into a micron-sized cluster with undefined shapes in aminated lignin, which were possibly induced by the freeze-drying process.⁴⁹

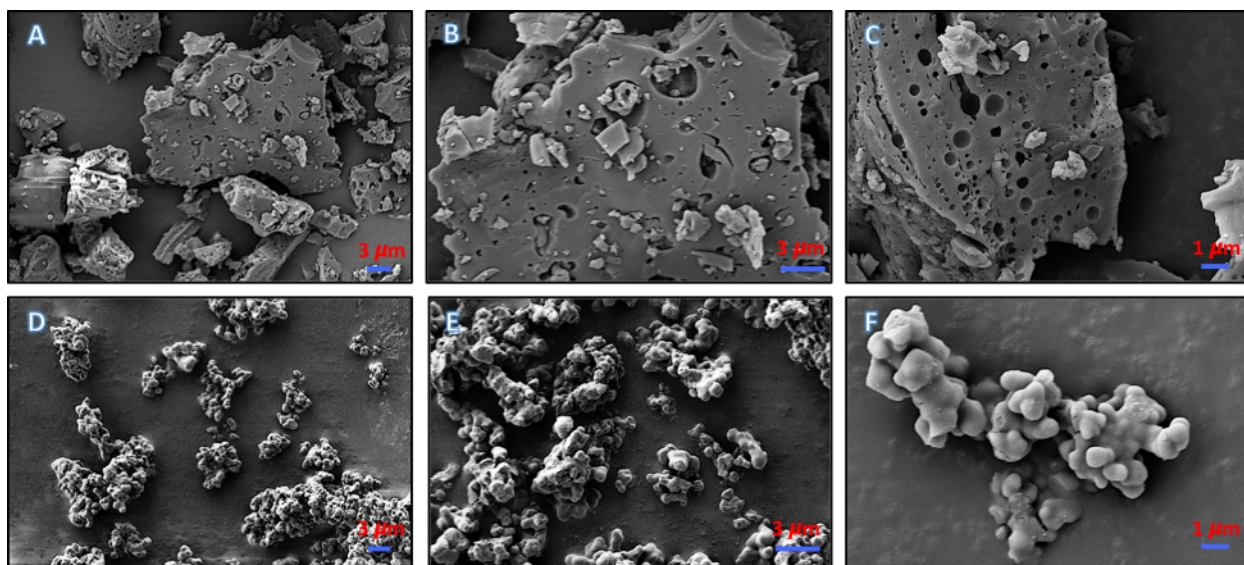


Figure 5. Scanning electron microscopy images of lignin (top) and aminated lignin (bottom). (A) and (D): Mag. = 5K; (B) and (E): Mag. = 10K; (C) and (F): Mag. = 20K.

Thermal gravimetric analysis. The first derivative of the thermogravimetric (DTG) curves of the original CELF lignin and its aminated products exhibited different thermal degradation stages in N_2 (Fig. 6). Overall, the aminated CELF lignin degraded faster than the unmodified lignin. In the pyrolysis range (200 °C to 600 °C), the DTG curve for CELF lignin exhibits a single decomposition step with a decomposition peak temperature of 395 °C, while the curve for the aminated CELF lignin exhibits two composition steps which are around 243 °C and 317 °C. The decomposition step above 300 °C is probably due to the cleavage of the C – C linkages and the demethoxylation of aromatic ring.^{37, 50} The lower degradation temperature for aminated lignin is probably due to the lower C – N bond energy compared to C – C bond. The decomposition step around 243 °C could be due to the degradation and evaporation of small molecular weight lignin fragments such as aliphatic side chains. The final degradation step

around 600 °C is probably due to the crack of C – C/H bond of the charcoal that was formed during the pyrolysis.⁵¹

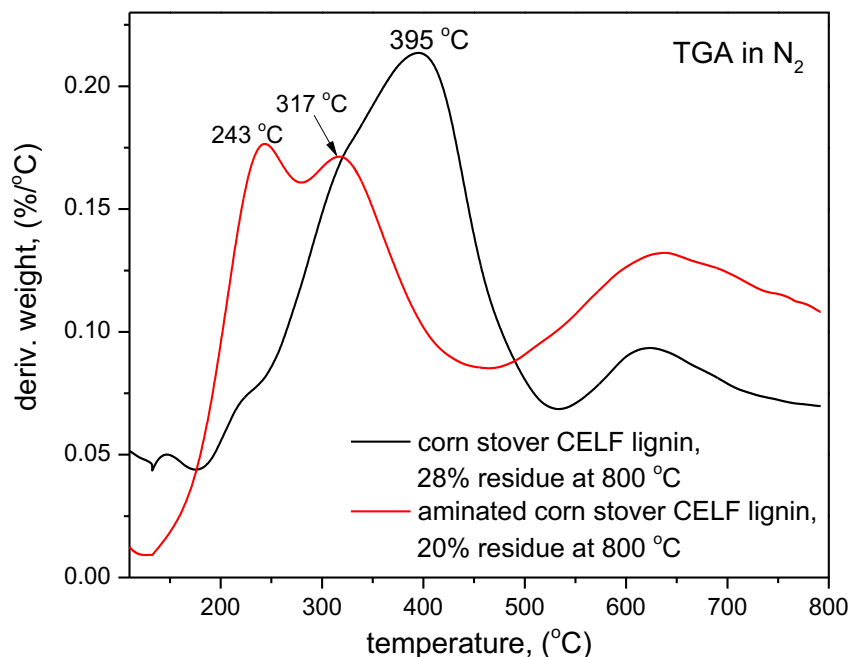


Figure 6. The derivative thermogravimetric curves of CELF lignin and aminated lignin.

BET surface area analysis. Table 2 summarizes the BET specific surface areas (S_{BET}) and BJH pore volumes (V_{BJH}) of the lignins before and after amination. Results indicated that the aminated lignin exhibited higher S_{BET} and V_{BJH} than those of the original CELF lignin. For example, the S_{BET} values were 4.2 and 5.9 m^2/g for CELF lignin and aminated lignin, respectively. In addition, the mesoporosity of these lignin samples is also confirmed by the pore size distribution analysis (Fig. S6). Since the aminated lignin had a larger surface area, it provided more adsorption sites and hence enhanced dye removal can be anticipated.

Table 2. Surface area and pore volume of CELF lignin and aminated lignin as determined by physisorption analysis.

Sample	BET surface area (m ² /g)	BJH pore volume (cm ³ /g)
CELF lignin	4.2	0.002
Aminated CELF lignin	5.9	0.006

Remove of dye by adsorbent. To demonstrate the potential dye-adsorption property of the modified CELF lignin, two types of dyes were tested in the lignin-dye adsorption experiment: a cationic dye MB and an anionic azo dye DB 1. The qualitative and quantitative effect of lignin loading on the dye decolorization efficiency for the original and aminated lignin is shown in Fig. 7. These results indicated that the aminated lignin showed drastically improved decolorization efficiency for both dyes especially the anionic DB 1 dye. For example, the amination process increased the DB 1 dye removal efficiency from <5% to >90% even at extremely low lignin loadings. The decolorization efficiency for MB dye is proportional to the dose of lignin, while no correlation could be obtained between the efficiency of DB 1 dye removal and the concentration of lignin. This might be attributed to the unmodified lignin's inability to adsorb DB 1 dye even at extremely high lignin dose and the aminated lignin's strong ability to adsorb DB 1 dye even at low lignin loadings. The effect of amino content on the adsorptivity of the aminated CELF lignin was further investigated, and the results indicated that the dye decolorization efficiency was positively correlated to the amino content of the modified CELF lignin (Fig. S7). The modified lignin has much higher decolorization efficiency toward the anionic dye (DB 1) compared to the cationic dye (MB). This could be mainly due to the electrostatic coupling between the cationic

side chain (amine group) of the aminated lignin and the anionic sites of the DB 1 dye.⁵² It is well known that pH affects the adsorption of most organic pollutants as well as the surface charges of adsorbents. To further confirm that electrostatic interactions is a key mechanism of adsorptive removal of dyes in DB 1 dye in aqueous solutions, the effect of initial pH on the dye decolorization efficiency and zeta potential of aminated CELF lignin was evaluated within the pH range of ~4.0 and 10.0 (Fig. 8). At extreme acidic or basic conditions (pH<3 or >12), lignin samples were found to be partially or completely dissolved in aqueous solutions, thus their adsorption and surface charge behaviors were not investigated at those conditions. These results also indicated that high pH values resulted in a decrease in the adsorptivity of aminated CELF lignin, which could be due to the increase of the magnitude of the negative zeta potential as pH increases. The aminated CELF lignin has a point of zero charge (pH_{PZC}) around 4.5, and its magnitude of zeta potential at each tested pH value (-2 to -25 mV) is significantly lower than that of the unmodified CELF lignin ranging from -68 to -75 mV (Fig. 8). This is due to the addition of the cationic amine group onto the side chain of aminated lignin. DB 1 dye has four sulfonate groups, thus it remains negatively charged at basic conditions and even at highly acidic solutions as these protonated sulfonate groups have a pK_a value lower than zero.⁵³ Therefore, the increase of the net negative zeta potential could further cause a decrease of the electrostatic interactions between the cationic lignin side chain and the negatively charged DB 1 dye in aqueous solution. This suggests that electrostatic force is a major interaction for DB 1 dye adsorption at lower pH. Furthermore, the decolorization efficiency is still above 60% even at high pH, although there

exists substantial electrostatic repulsion between the modified lignin and DB 1 dye. This indicates that mechanisms other than electrostatic interaction such as hydrogen bonding and π - π stacking are also operative for the DB 1 dye adsorption on the aminated CELF lignin.⁵⁴ On the other hand, hydrogen bonding, π -interaction, and limited electrostatic interaction between lignin dissociated carboxyl/hydroxyl groups and the cationic sites of the dye molecule are believed to be responsible for the MB dye adsorption.¹ Fig. 9 shows a proposed scheme for the MB and DB 1 dye binding to the unmodified CELF lignin and aminated lignin surface.

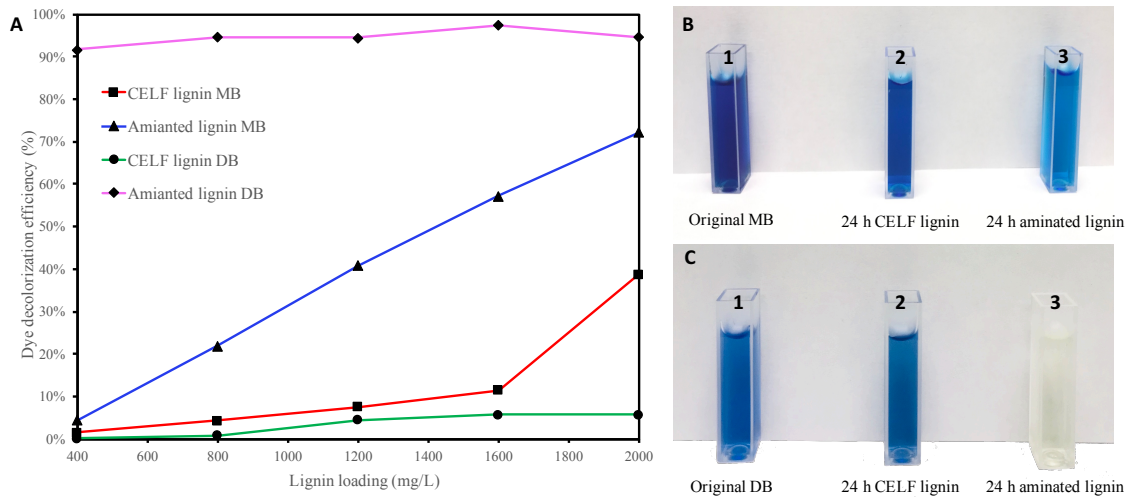


Figure 7. Dye adsorption capacity of the CELF lignin and aminated lignin. (A). The effect of lignin loading on dye decolorization efficiency. (B). MB dye before (1) and after (2,3) 24 h lignin adsorption. (C). DB 1 dye before (1) and after (2,3) 24 h lignin adsorption.

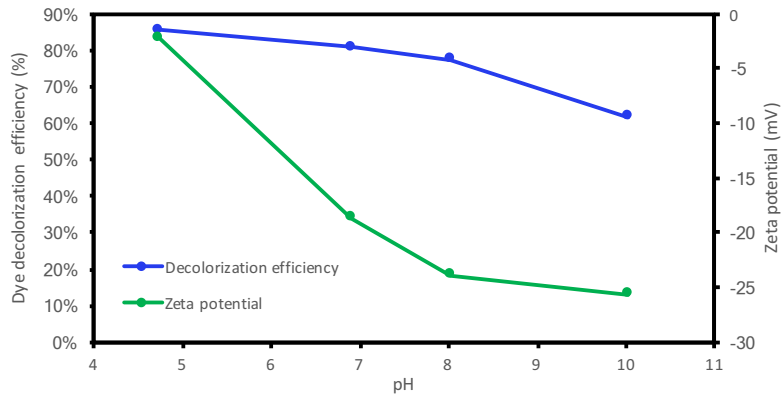


Figure 8. The effect of pH on the zeta potential and adsorptivity of the modified lignin toward direct blue dye.

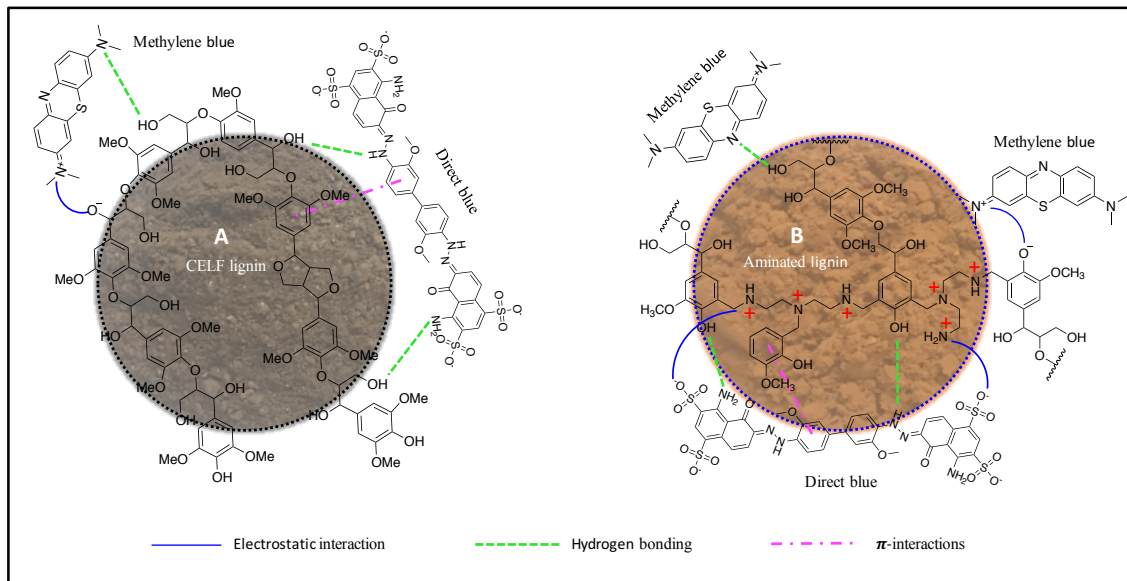


Figure 9. A proposed scheme of Direct blue and Methylene blue dye binding to the CELF lignin (A) and aminated lignin (B).

The Langmuir and Freundlich model were used to study the adsorption isotherms of azo-dyes, and their equations (Eq. 1 and 2) are shown below:

$$\frac{C_e}{Q_e} = \frac{C_e}{Q_m} + \frac{1}{Q_m K_L} \quad (1)$$

$$\log Q_e = \log K_F + \frac{1}{n} \log C_e \quad (2)$$

where c_e (mg/mL) is the equilibrium concentration, Q_e (mg/g) is the equilibrium adsorption capacity, Q_m (mg/g) is the maximum adsorption capacity of the Langmuir isotherm model, K_L (mL/mg) is a Langmuir adsorption coefficient, K_F (mL/mg) is the Freundlich constant, and $1/n$ is an indicator that reflects the nonlinear degree of adsorption. Fig. 10 shows the Langmuir (A) and Freundlich (C) adsorption isotherms curves, and the linear analysis (B and D) indicated that the observed dye adsorption data for aminated CELF lignin were better described by the Langmuir isotherm model as confirmed by the higher coefficient R^2 . The Langmuir fitting results suggested that the adsorption process between lignin and the azo dye could be characterized as a monolayer type of adsorption. The Langmuir isotherm analysis indicated that the maximum adsorption capacity of the aminated CELF lignin is 502.7 mg/g for DB 1 dye. A direct comparison of the maximum adsorption capacities of different anionic azo dyes on various previously reported adsorbents is presented in Table 3. Based on our literature survey, it was found that the adsorption capacity of aminated CELF lignin is higher than that of all other adsorbents except carbon nanospheres. It should be noted that these adsorbents include commercial activated carbon, anion exchange membrane, and multi-wall-carbon nanotubes which are all well-known for their high aspect ratio, natural porosity, and strong ability to adsorb pollutants from aqueous system. This suggests that the aminated CELF lignin, as a low-cost renewable resource, is highly suitable for the removal of azo-dyes from the aqueous solutions.

Table 3. The adsorption performance of different adsorbents towards azo-dyes as characterized by the maximum adsorption capacity (mg dye/g substrate)

Adsorbent	Dye adsorbate	Maximum Capacity (mg/g)	Reference
Granular activated carbon	Congo Red	9.1	55
Zeolite	Direct Blue 71	13.7	6
Graphene oxide	Acid Orange 8	29.0	11
Chitosan Halloysite Nanotubes	Congo Red	41.5	56
Multi-wall-carbon nanotube	Tartrazine	84.0	57
Mn _{0.4} Zn _{0.6} Fe ₂ O ₄ nanoparticles	Tartrazine	90.8	58
Mn _{0.4} Zn _{0.6} Fe ₂ O ₄ nanoparticles	Ponceau 4R	101.4	58
SEG modified starch	Direct Red 23	129.9	59
SEG modified starch	Acid Blue 92	147.1	59
Lignin amine coated Fe ₃ O ₄	Acid scarlet GR	176.5	54
Chitosan	Tartrazine	350	60
Multi-wall-carbon nanotube	Direct Blue 53	409.4	53
Graphene oxide sponge	Direct red 80	501.3	5
Aminated CELF lignin	Direct Blue 1	502.7	Present
Chitosan-based hydrogel	Erichrome black T	520	61
Carbon nanospheres	Acid Red 88	555.6	62
Fe(OH) ₃ @Cellulose hybrid fibers	Congo Red	689.7	63

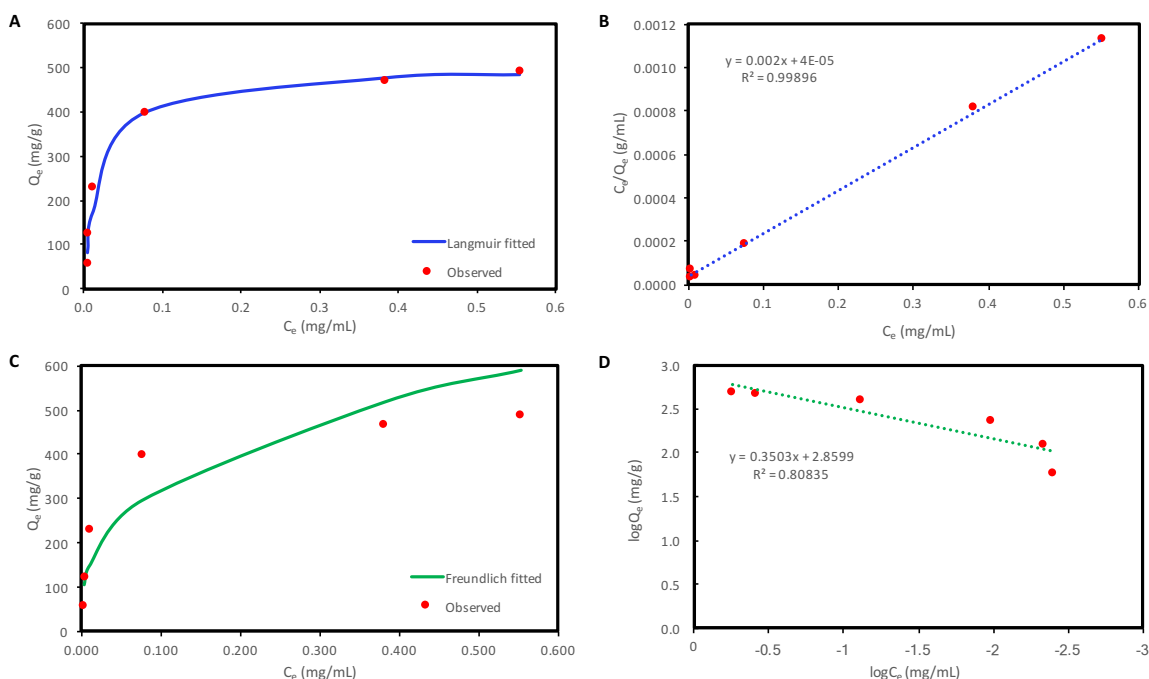


Figure 10. Adsorption isotherms of Direct blue 1 by aminated CELF lignin. (A) Langmuir fitted adsorption isotherm curve; (B) The linear fit of Langmuir model ($R^2 = 0.99$); (C) Freundlich fitted adsorption isotherm curve; (D) The linear fit of La Freundlich model ($R^2 = 0.81$).

The rate of the adsorption process is an important factor that determines if the sorbent could be used on large scales in industrial applications, and it can be determined by kinetic studies. In the study of solid-liquid static adsorption kinetics, the relationship between the time and the amount of adsorption is typically fitted through dynamic models.⁶⁴ Two mathematical models are usually adapted to analyze the dynamic models of adsorption process, namely pseudo first-order (Eq. 3) and pseudo second-order (Eq. 4) equation:

$$\log(Q_e - Q_t) = \log Q_e - \frac{K_1 t}{2.303} \quad (3)$$

$$\frac{t}{Q_t} = \frac{t}{Q_e} + \frac{1}{Q_e^2 K_2} \quad (4)$$

where Q_e and Q_t are adsorption capacity (mg/g) at equilibrium time and any instant of adsorption time t (min), K_1 and K_2 are the rate constant of the pseudo-first-order and second-order adsorption, respectively. The study about the effect of time on the adsorption process, as shown in Fig. S8, suggests that the amount of dye adsorbed by the adsorbent increases rapidly at the beginning for 30 min, and then the adsorption efficiency becomes slow for 240 min until the adsorption equilibrium is reached. The pseudo first and second kinetic models assume that the adsorption process is governed by diffusion and chemical adsorption mechanism, respectively. The observed experimental data were fitted to the pseudo-first-order and second-order equations, and their linear fitted plots and the parameters of the kinetic model were shown in Fig. 11 and

Table 4, respectively. It was found that the correlation coefficient (R^2) of pseudo second-order equation kinetic model was higher than that of the pseudo-first-order model, suggesting the pseudo-second-order kinetic model may be more suitable for describing the kinetics of the adsorption process of the DB 1 dye on the aminated CELF lignin. This suggested that the adsorption behaviors of azo-dye onto the modified lignin are dominated by chemical adsorption instead of diffusion process. It has been reported that the adsorption process is generally divided into three main stages, including film diffusion stage, Intraparticle diffusion stage, and the final actual adsorption stage.⁶⁵ To further test if the intraparticle diffusion is the only rate determining step of the adsorption process, the intraparticle diffusion kinetic model is also fitted with the experimental data (Fig. S9), and results indicated that the adsorption process has more than one speed controlling step. In addition, the relatively large boundary layer thickness as reflected by the large intercept of the linear plot ($t^{1/2}$ vs. q_t) suggests that membrane diffusion might also have a great effect on the adsorption process.⁶⁵

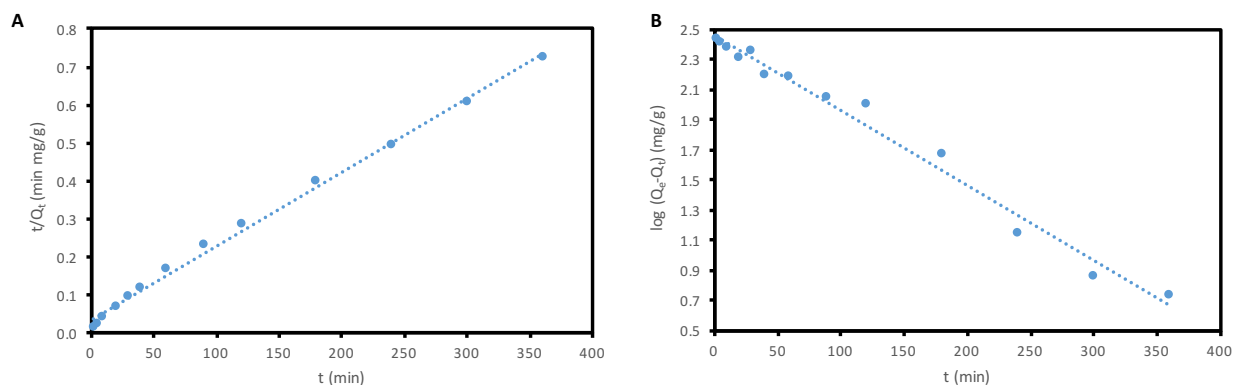


Figure 11. Pseudo-second order plot (A) and Pseudo-first order plot (B) for the Direct blue dye adsorption kinetics by aminated CELF lignin.

Table 4. Parameters of adsorption kinetic model.

Kinect model	q_e (mg g ⁻¹)	K_1 (min ⁻¹) or K_2 (g mg ⁻¹ min ⁻¹)	R^2
Pseudo-first order	285.8	0.01152	0.984
Pseudo-second order	511.7	0.00013	0.996

Reusability of the adsorbent represents an important aspect to minimize the cost of the overall adsorption process. The recycle performances of aminated CELF lignin for DB 1 dye removal were also investigated in this study. The results, as shown in Fig. 12, show that no significant reduction in the adsorption efficiency is found for three cycles compared with that of the fresh adsorbent, although there is a gradual decrease in the dye removal efficiencies possibly due to the incomplete of dye desorption. The dye removal efficiency decreased to 65% for the fourth use, probably due to the saturation of the adsorbent surface. Thus, the recycle study demonstrated that the aminated CLEF lignin remained as an efficient adsorbent even after multiple reuses.

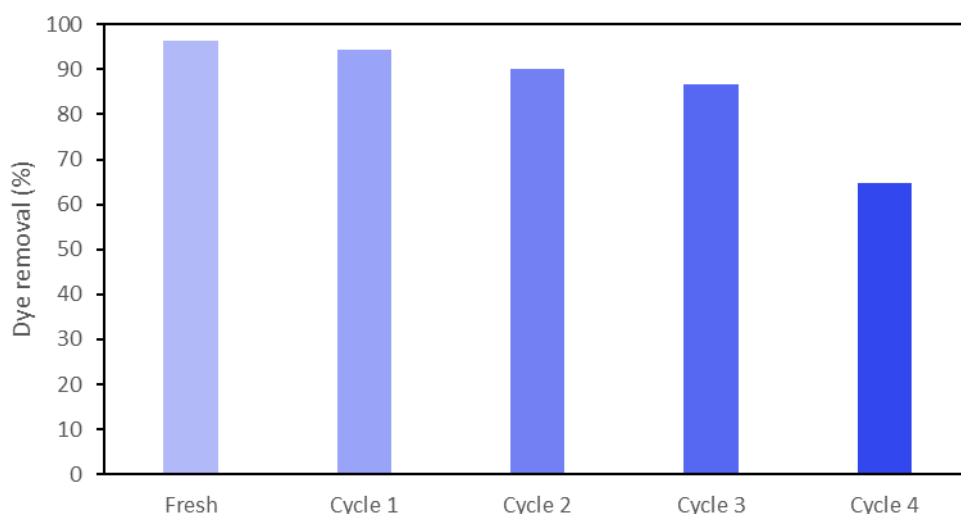


Figure 12. The removal efficiency of aminated CELF lignin for DB 1 dye after four adsorption-desorption cycles.

Aminated CELF lignin characterization after dye adsorption. The FTIR spectra of aminated CELF lignin before and after dye adsorption are shown in Fig. S10. After adsorption, two additional peaks at around 1200 and 1035 cm^{-1} representing the stretching vibration bands of the sulfonate group appear in the aminated lignin due to the attachment of the DB 1 dye. The N=N stretching vibration from DB 1 dye is unclear in the IR spectra since the direct dye is a symmetrical trans azo compound. SEM was also used to analyze the morphology of the aminated CELF lignin's surface after the adsorption of DB 1 dye (Fig. 13). Results showed that the shape of lignin particles did not change dramatically and remained as an aggregated cluster with irregular shapes and heterogeneous surface, but their size appeared to increase significantly after dye adsorption. These observations clearly revealed that the DB 1 dye is adsorbed on the surface of the modified CELF lignin.

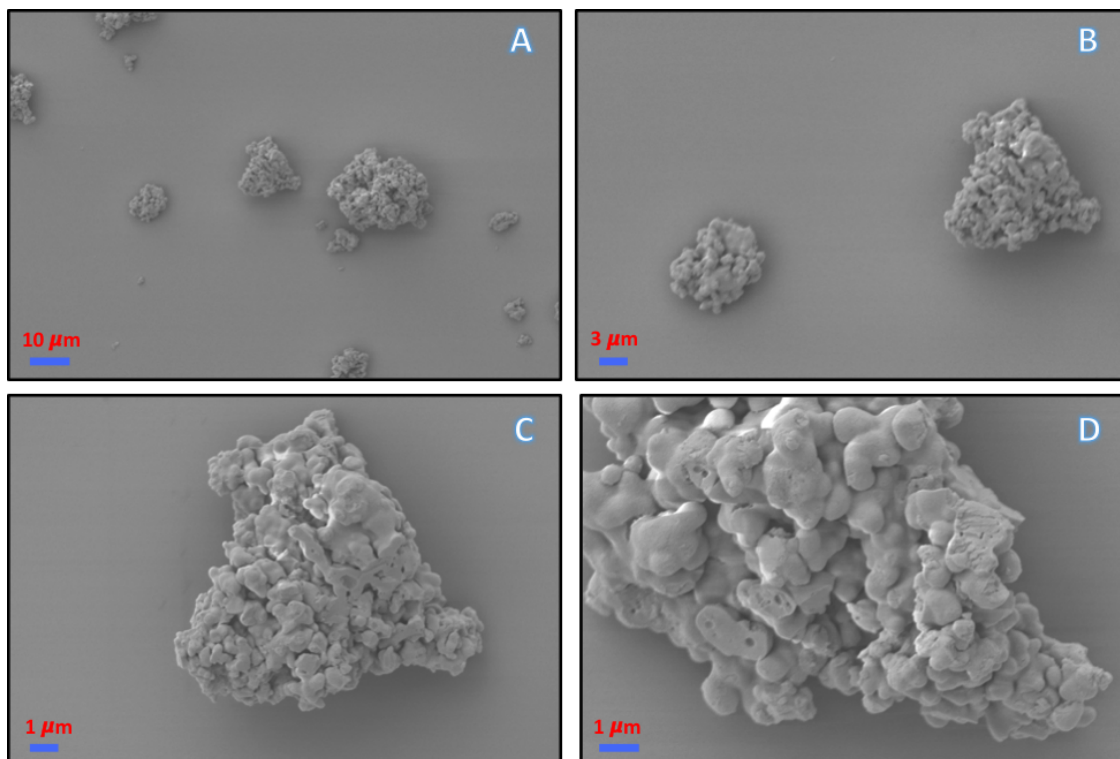


Figure 13. SEM images of aminated lignin after adsorption of DB 1 dye. (A. Mag. = 2K. B. Mag. = 5K. C. Mag. = 10K. D. Mag. = 20K.)

CONCLUSIONS

Development of low-cost renewable bio-adsorbents for removal of toxic dyes from contaminated water has been a topic of great interest but remains challenging. In this study, aminated corn stover lignin was synthesized via combinatorial CELF pretreatment and Mannich reaction to remove azo dyes from aqueous solutions. Under acid conditions, both the primary and secondary amines have high reactivity toward the H_{3/5} and G₅ position of CELF lignin. SEM revealed that the original lignin particles are distributed in a large conglomerate, while the surface of aminated lignin becomes smoother and the nano-spheric particles of the modified lignin aggregate into nano- and micron-sized cluster with undefined shapes. The combination of CELF pretreatment and Mannich reaction significantly increased the adsorption behavior of aminated lignin toward azo direct blue 1 dye with a maximum capacity of 502.7 mg/g, which is significantly higher than that of many adsorbent materials reported in the literature. Recycle studied suggested that once recovered, the bio-adsorbent was capable of maintaining a relatively high dye removal efficiency (>85%) even after three recycles. In conclusion, the proposed aminated CELF lignin could be considered as a cost-effective bio-adsorptive platform for the efficient removal of azo dyes from aqueous solutions.

EXPERIMENTAL SECTION

Feedstocks and Chemicals. Kramer corn stover was provided by the National Renewable Energy Laboratory (NREL, Golden, CO). The corn stover was knife milled to pass through a 1 mm particle size interior sieve using a laboratory mill (Model 4, Arthur H. Thomas Company, Philadelphia, PA). All the chemicals used in this study were used as received from Sigma-Aldrich without any further purification.

Production of CELF lignin. CELF pretreatment of corn stover was performed in a custom built 1 L Hastelloy Parr reactor (Parr instruments Company, Moline, IL) at 7.5 wt% solids loading and 0.5wt% H₂SO₄ acid loading. The CELF reaction was sustained at 180 °C for 25 min in an equivolume mixture of THF and water. After pretreatment, the reactor was quenched in a 25 °C water bath and the liquid phase was separated from the pretreated solids through vacuum paper filtration. CELF lignin was then isolated from the liquid phase by first neutralization with ammonium hydroxide followed by THF evaporation and subsequent vacuum filtration of the precipitated lignin from the neutralized liquor. The obtained CELF lignin was washed with water and diethyl ether and dried at 45°C in an incubator. Once dried, the lignin was finally crushed to a fine powder in a mortar & pestle and stored in a container prior to further test and modification.

Amination of CELF lignin. Corn stover CELF lignin (~200 mg) was mixed with 2 mL of dioxane in a round-flask under constant stirring for 20 min at room temperature until the lignin was fully dissolved. Specified amounts of DETA, acetic acid, and formaldehyde were then added into the solution with continuous stirring. Formaldehyde was added stepwise to avoid unnecessary crosslinking reactions. Subsequently, the flask was heated in a sand bath, kept at a

specified temperature (45, 60, 75, and 90 °C) and stirred for a specified time (1, 2, 3, and 4 h). Afterward, the reaction mixture was evaporated under reduced pressure to remove the majority of the organic solvent followed by dialysis with a molecular weight cut off of 1000 Da. The obtained aminated CELF lignin was finally freeze-dried and store at room temperature before further characterization.

Lignin characterization before and after amination. *FTIR analysis.* The IR spectra were collected using a Spectrum One FTIR spectrophotometer (PerkinElmer, Wellesley, MA) equipped with a diamond-composite attenuated total reflectance (ATR) cell from 1000 to 4000 cm^{-1} with 128 scans at 4 cm^{-1} resolutions.

NMR analysis. NMR experiments were acquired with a Bruker Avance III HD 500 MHz spectrometer equipped with a 5 mm N_2 cryogenically cooled BBO H&F probe according to previously published literatures.^{32, 66} A standard Bruker pulse sequence (hsqcetgpspsi2.2) and an inverse-gated decoupling pulse sequence (Waltz-16) were applied for HSQC and ^{31}P NMR experiment, respectively.

SEM analysis. The morphology of lignin samples was observed with a scanning electron microscopy (SEM, Zeiss Auriga, Germany) at an accelerating voltage of 5 kV. The samples were sputter-coated with Au using an SPI-Module Sputter Coater for 50 s. Imaging was subsequently captured at various magnifications from 2K to 20K.

Thermal gravimetric analysis. The TGA was performed by a TGA Q50 thermo-gravimetric analyzer (TA instruments, UDA). Lignin samples (~5 mg) were loaded to a Platinum

sample pan (TA instruments) and heated in nitrogen from 25 to 105 °C at 20 °C/min. After incubating at 105 °C for 10 min, it was heated further from 105 to 800 °C at a heating rate of 20 °C/min.

Zeta potential analysis. The zeta potential of lignin suspensions was measured at different hydrogen ion concentrations while keeping a concentration of 1 mg/mL, using a ZetaPALS (Brookhaven Instruments Corporation, NY). The mean zeta potential of each suspension were calculated from 10 measurements.

Surface area and pore size analysis. The N₂ adsorption-desorption measurement of samples was carried out at 77 K on a Quantachrome Autosorb iQ. The samples were first degassed at 353K for ~17 h before being loaded into the analysis station. The pore volume and pore size distribution were determined using a Barrett–Joyner–Halenda (BJH) method. The specific surface area was calculated using Brunauer–Emmett–Teller (BET) in the P/P0 range of 0.05–0.30.

Dye decolorization study. Various amounts of CELF lignin and aminated lignin were mixed with 25 mL of MB or DB 1 dye solution with a concentration of 50 mg/L. The mixture was left in an incubator at 25 °C and 150 rpm for 24 h. The concentration of dye in the supernatant of the solution at the equilibrium was determined by a UV spectrophotometer. The amount of dye adsorbed (q_e) by lignin substrates was calculated based on the following Equation 5:

$$q_e = \frac{v(C_0 - C_e)}{m} \quad (5)$$

where c_o and c_e represent the initial and equilibrium concentrations of dye solution (mg/L), respectively. v is the volume of the total solution (mL), and m is the dry weight of the lignin sample (g). The maximum wavelength for MB and DB 1 dye was set at 663 and 624 nm, respectively. The extinction coefficient of MB and DB 1 dye was determined to be 149.3 and 12.3 L mol⁻¹ cm⁻¹ based on the Beer's law calibration (Fig. S1 and S2). The decolorization efficiency (η) is defined by:

$$\eta = \frac{c_o - c}{c_o} \times 100\% \quad (6)$$

where c_o represents the initial concentration, and c is the concentration of dye in the supernatant after decolorization. The adsorption isotherms of DB 1 dye onto aminated lignin were measured with varying concentrations of dye ranging from 0.05 to 1 mg/mL at 25 °C. To further investigate the kinetics of dye adsorption, the equilibrium concentrations of dye solution were measured from 5 min to 8 h after mixing 20 mg of aminated lignin with 40 mL of DB 1 with an initial concentration of 1 mg/mL. The effect of initial pH on dye adsorption was studied by mixing ~10 mg of lignin with 25 mL of initial DB 1 dye with a concentration of 50 mg/mL at 25 °C. ~0.1M HNO₃ and 0.01M of NaOH were used to adjust the pH between 4 and 10. For recycling experiment, dilute NaOH (pH=10) was used to release the adsorbed dye from adsorbent. The adsorption of the dye by the regenerated lignin was repeated four times by mixing ~20 mg of solid with 25 mL of MB or DB 1 dye solution with a concentration of 50 mg/L.

ASSOCIATED CONTENT

Supporting Information

The Supporting Information is available free of charge on the ACS Publications website at DOI:

Calibration curve of dyes; schematic diagram of Mannich reaction; Ninhydrin test of lignin amination; Phosphitylation reactions between lignin OHs and TMDP; pore size distribution of lignin samples; effect of amino content on the adsorptivity of aminated CELF lignin; Effect of contact time on adsorption; Intraparticle diffusion kinetic of DB 1 dye; FTIR spectra of the aminated CELF lignin before and after dye adsorption.

AUTHOR INFORMATION

Corresponding Author

*Xianzhi Meng, E-mail: xmeng5@utk.edu

*Art J. Ragauskas, E-mail: argauskas@utk.edu

Authors' Contributions

The experiments were performed through contributions of all authors. All authors have approved the final version of the manuscript.

Notes

The authors declare that they have no competing financial interests.

ACKNOWLEDGMENTS

This work is supported by “Agriculture and Food Research Initiative - Sustainable Bioenergy and Bioproducts Challenge Area” [grant no. USDA-NIFA-AFRI-006352/project accession no. 1015189] from the U.S. Department of Agriculture (USDA) National Institute of Food and Agriculture (NIFA). Facilities at UC Riverside were provided by the Bourns' College of

Engineering Center for Environmental Research & Technology (CE-CERT). We also want to thank Sarah Humphries from University of Tennessee - Knoxville for her administrative support including help us purchasing all the suppliers for the study.

REFERENCES

1. Budnyak, T. M.; Aminzadeh, S.; Pylypchuk, I. V.; Sternik, D.; Tertykh, V. A.; Lindström, M. E.; Sevastyanova, O., Methylene Blue dye sorption by hybrid materials from technical lignins. *Journal of Environmental Chemical Engineering* **2018**, *6* (4), 4997-5007.
2. Abdelhamid, H. N.; Zou, X., Template-free and room temperature synthesis of hierarchical porous zeolitic imidazolate framework nanoparticles and their dye and CO₂ sorption. *Green Chemistry* **2018**, *20* (5), 1074-1084.
3. Wang, S.; Kong, F.; Fatehi, P.; Hou, Q., Cationic High Molecular Weight Lignin Polymer: A Flocculant for the Removal of Anionic Azo-Dyes from Simulated Wastewater. *Molecules* **2018**, *23* (8), 2005.
4. Peng, N.; Hu, D.; Zeng, J.; Li, Y.; Liang, L.; Chang, C., Superabsorbent Cellulose–Clay Nanocomposite Hydrogels for Highly Efficient Removal of Dye in Water. *ACS Sustainable Chemistry & Engineering* **2016**, *4* (12), 7217-7224.
5. Zambare, R.; Song, X.; Bhuvana, S.; Antony Prince, J. S.; Nemade, P., Ultrafast Dye Removal Using Ionic Liquid–Graphene Oxide Sponge. *ACS Sustainable Chemistry & Engineering* **2017**, *5* (7), 6026-6035.
6. Mirzaei, N.; Mahvi, A. H.; Hossini, H., Equilibrium and kinetics studies of Direct blue 71 adsorption from aqueous solutions using modified zeolite. *Adsorption Science & Technology* **2018**, *36* (1-2), 80-94.
7. Sohni, S.; Hashim, R.; Nidaullah, H.; Lamaming, J.; Sulaiman, O., Chitosan/nano-lignin based composite as a new sorbent for enhanced removal of dye pollution from aqueous solutions. *Int. J. Biol. Macromol.* **2019**, *132*, 1304-1317.
8. Zhang, L.; Lu, H.; Yu, J.; McSporran, E.; Khan, A.; Fan, Y.; Yang, Y.; Wang, Z.; Ni, Y., Preparation of High-Strength Sustainable Lignocellulose Gels and Their Applications for Antiultraviolet Weathering and Dye Removal. *ACS Sustainable Chemistry & Engineering* **2019**, *7* (3), 2998-3009.
9. Singh, S.; Sidhu, G. K.; Singh, H., Removal of methylene blue dye using activated carbon prepared from biowaste precursor. *Indian Chemical Engineer* **2019**, *61* (1), 28-39.
10. Oliveira, E. H. C. d.; Marques Fraga, D. M. d. S.; da Silva, M. P.; Fraga, T. J. M.; Carvalho, M. N.; de Luna Freire, E. M. P.; Ghislandi, M. G.; da Motta Sobrinho, M. A., Removal of toxic dyes from aqueous solution by adsorption onto highly recyclable xGnP® graphite nanoplatelets. *Journal of Environmental Chemical Engineering* **2019**, *7* (2), 103001.

11. Konicki, W.; Aleksandrak, M.; Moszyński, D.; Mijowska, E., Adsorption of anionic azo-dyes from aqueous solutions onto graphene oxide: Equilibrium, kinetic and thermodynamic studies. *J. Colloid Interface Sci.* **2017**, *496*, 188-200.
12. Mahmoodi, N. M.; Ghezelbash, M.; Shabani, M.; Aryanasab, F.; Saeb, M. R., Efficient removal of cationic dyes from colored wastewaters by dithiocarbamate-functionalized graphene oxide nanosheets: From synthesis to detailed kinetics studies. *Journal of the Taiwan Institute of Chemical Engineers* **2017**, *81*, 239-246.
13. Alatalo, S.-M.; Mäkilä, E.; Repo, E.; Heinonen, M.; Salonen, J.; Kukk, E.; Sillanpää, M.; Titirici, M.-M., Meso- and microporous soft templated hydrothermal carbons for dye removal from water. *Green Chemistry* **2016**, *18* (4), 1137-1146.
14. Ragauskas, A. J.; Williams, C. K.; Davison, B. H.; Britovsek, G.; Cairney, J.; Eckert, C. A.; Frederick, W. J., Jr.; Hallett, J. P.; Leak, D. J.; Liotta, C. L.; Mielenz, J. R.; Murphy, R.; Templer, R.; Tschaplinski, T., The path forward for biofuels and biomaterials. *Science (Washington, DC, U. S.)* **2006**, *311* (5760), 484-489.
15. Amore, A.; Ciesielski, P. N.; Lin, C.-Y.; Salvachúa, D.; Sánchez i Nogué, V., Development of Lignocellulosic Biorefinery Technologies: Recent Advances and Current Challenges. *Aust. J. Chem.* **2016**, *69* (11), 1201-1218.
16. Ragauskas, A. J.; Beckham, G. T.; Biddy, M. J.; Chandra, R.; Chen, F.; Davis, M. F.; Davison, B. H.; Dixon, R. A.; Gilna, P.; Keller, M.; Langan, P.; Naskar, A. K.; Saddler, J. N.; Tschaplinski, T. J.; Tuskan, G. A.; Wyman, C. E., Lignin Valorization: Improving Lignin Processing in the Biorefinery. *Science* **2014**, *344* (6185), 1246843.
17. Langholtz, M.; Downing, M.; Graham, R.; Baker, F.; Compere, A.; Griffith, W.; Boeman, R.; Keller, M., Lignin-Derived Carbon Fiber as a Co-Product of Refining Cellulosic Biomass. *SAE Int. J. Mater. Manf.* **2014**, *7*, 115-121.
18. Gillet, S.; Aguedo, M.; Petitjean, L.; Morais, A. R. C.; da Costa Lopes, A. M.; Lukasik, R. M.; Anastas, P. T., Lignin transformations for high value applications: towards targeted modifications using green chemistry. *Green Chemistry* **2017**, *19* (18), 4200-4233.
19. Gadioli, R.; Waldman, W. R.; De Paoli, M. A., Lignin as a green primary antioxidant for polypropylene. *J. Appl. Polym. Sci.* **2016**, *133* (45).
20. Liu, L.; Qian, M.; Song, P. a.; Huang, G.; Yu, Y.; Fu, S., Fabrication of Green Lignin-based Flame Retardants for Enhancing the Thermal and Fire Retardancy Properties of Polypropylene/Wood Composites. *ACS Sustainable Chemistry & Engineering* **2016**, *4* (4), 2422-2431.
21. Yu, C.; Wang, F.; Zhang, C.; Fu, S.; Lucia, L. A., The synthesis and absorption dynamics of a lignin-based hydrogel for remediation of cationic dye-contaminated effluent. *React. Funct. Polym.* **2016**, *106*, 137-142.
22. Domínguez-Robles, J.; Peresin, M. S.; Tamminen, T.; Rodríguez, A.; Larrañeta, E.; Jääskeläinen, A.-S., Lignin-based hydrogels with “super-swelling” capacities for dye removal. *Int. J. Biol. Macromol.* **2018**, *115*, 1249-1259.

23. Andradý, A. L.; Pandey, K. K.; Heikkilä, A. M., Interactive effects of solar UV radiation and climate change on material damage. *Photochemical & Photobiological Sciences* **2019**, *18* (3), 804-825.
24. Figueiredo, P.; Lintinen, K.; Hirvonen, J. T.; Kostianen, M. A.; Santos, H. A., Properties and chemical modifications of lignin: Towards lignin-based nanomaterials for biomedical applications. *Prog. Mater. Sci.* **2018**, *93*, 233-269.
25. Buono, P.; Duval, A.; Verge, P.; Averous, L.; Habibi, Y., New Insights on the Chemical Modification of Lignin: Acetylation versus Silylation. *ACS Sustainable Chemistry & Engineering* **2016**, *4* (10), 5212-5222.
26. Liu, Z.; Zhao, L.; Cao, S.; Wang, S.; Li, P., Preparation and Evaluation of a Novel Cationic Amphiphilic Lignin Derivative with High Surface Activity. *2013* **2013**, *8* (4), 10.
27. Ye, X.-X.; Luo, W.; Lin, L.; Zhang, Y.-q.; Liu, M.-h., Quaternized lignin-based dye dispersant: Characterization and performance research. *J. Dispersion Sci. Technol.* **2017**, *38* (6), 852-859.
28. Ge, Y.; Song, Q.; Li, Z., A Mannich base biosorbent derived from alkaline lignin for lead removal from aqueous solution. *Journal of Industrial and Engineering Chemistry* **2015**, *23*, 228-234.
29. Tao, X.; Shi, L. S.; Sun, M. J.; Li, N., Synthesis of Lignin Amine Asphalt Emulsifier and its Investigation by Online FTIR Spectrophotometry. *Advanced Materials Research* **2014**, *909*, 72-76.
30. Liu, Z.; Lu, X.; An, L.; Xu, C., A Novel Cationic Lignin-amine Emulsifier with High Performance Reinforced via Phenolation and Mannich Reactions. *2016* **2016**, *11* (3), 14.
31. Seemala, B.; Meng, X.; Parikh, A.; Nagane, N.; Kumar, R.; Wyman, C. E.; Ragauskas, A.; Christopher, P.; Cai, C. M., Hybrid Catalytic Biorefining of Hardwood Biomass to Methylated Furans and Depolymerized Technical Lignin. *ACS Sustainable Chemistry & Engineering* **2018**, *6* (8), 10587-10594.
32. Meng, X.; Parikh, A.; Seemala, B.; Kumar, R.; Pu, Y.; Wyman, C. E.; Cai, C. M.; Ragauskas, A. J., Characterization of fractional cuts of co-solvent enhanced lignocellulosic fractionation lignin isolated by sequential precipitation. *Bioresour. Technol.* **2019**, *272*, 202-208.
33. Ataefard, M.; Shadman, A.; Saeb, M. R.; Mohammadi, Y., A hybrid mathematical model for controlling particle size, particle size distribution, and color properties of toner particles. *Appl. Phys. A* **2016**, *122* (8), 726.
34. Hosseinnzhad, M.; Shadman, A.; Saeb, M. R.; Mohammadi, Y., A new direction in design and manufacture of co-sensitized dye solar cells: Toward concurrent optimization of power conversion efficiency and durability. *Opto-Electronics Review* **2017**, *25* (3), 229-237.
35. Du, X.; Li, J.; Lindström, M. E., Modification of industrial softwood kraft lignin using Mannich reaction with and without phenolation pretreatment. *Industrial Crops and Products* **2014**, *52*, 729-735.

36. Zhou, W.; Chen, F.; Zhang, H.; Wang, J., Preparation of a Polyhydric Aminated Lignin and Its Use in the Preparation of Polyurethane Film. *J. Wood Chem. Technol.* **2017**, *37* (5), 323-333.
37. Jiao, G.-J.; Peng, P.; Sun, S.-L.; Geng, Z.-C.; She, D., Amination of biorefinery technical lignin by Mannich reaction for preparing highly efficient nitrogen fertilizer. *Int. J. Biol. Macromol.* **2019**, *127*, 544-554.
38. Qiao, X.; Zhao, C.; Shao, Q.; Hassan, M., Structural Characterization of Corn Stover Lignin after Hydrogen Peroxide Pre-soaking Prior to Ammonia Fiber Expansion Pretreatment. *Energy & Fuels* **2018**, *32* (5), 6022-6030.
39. Wang, X.; Zhang, Y.; Hao, C.; Dai, X.; Zhou, Z.; Si, N., Ultrasonic-assisted synthesis of aminated lignin by a Mannich reaction and its decolorizing properties for anionic azo-dyes. *RSC Advances* **2014**, *4* (53), 28156-28164.
40. Chatterjee, M.; Ishizaka, T.; Kawanami, H., Reductive amination of furfural to furfurylamine using aqueous ammonia solution and molecular hydrogen: an environmentally friendly approach. *Green Chemistry* **2016**, *18* (2), 487-496.
41. Constant, S.; Wienk, H. L. J.; Frissen, A. E.; Peinder, P. d.; Boelens, R.; van Es, D. S.; Grisel, R. J. H.; Weckhuysen, B. M.; Huijgen, W. J. J.; Gosselink, R. J. A.; Bruijninx, P. C. A., New insights into the structure and composition of technical lignins: a comparative characterisation study. *Green Chemistry* **2016**, *18* (9), 2651-2665.
42. Meng, X.; Evans, B. R.; Yoo, C. G.; Pu, Y.; Davison, B. H.; Ragauskas, A. J., Effect of in Vivo Deuteration on Structure of Switchgrass Lignin. *ACS Sustainable Chemistry & Engineering* **2017**, *5* (9), 8004-8010.
43. Yoo, C. G.; Li, M.; Meng, X.; Pu, Y.; Ragauskas, A. J., Effects of organosolv and ammonia pretreatments on lignin properties and its inhibition for enzymatic hydrolysis. *Green Chemistry* **2017**, *19* (8), 2006-2016.
44. Sun, S.; Huang, Y.; Sun, R.; Tu, M., The strong association of condensed phenolic moieties in isolated lignins with their inhibition of enzymatic hydrolysis. *Green Chemistry* **2016**, *18* (15), 4276-4286.
45. Wang, X.; Guo, Y.; Zhou, J.; Sun, G., Structural changes of poplar wood lignin after supercritical pretreatment using carbon dioxide and ethanol-water as co-solvents. *RSC Advances* **2017**, *7* (14), 8314-8322.
46. Wildschut, J.; Smit, A. T.; Reith, J. H.; Huijgen, W. J. J., Ethanol-based organosolv fractionation of wheat straw for the production of lignin and enzymatically digestible cellulose. *Bioresour. Technol.* **2013**, *135*, 58-66.
47. Meng, X.; Parikh, A.; Seemala, B.; Kumar, R.; Pu, Y.; Christopher, P.; Wyman, C. E.; Cai, C. M.; Ragauskas, A. J., Chemical Transformations of Poplar Lignin during Cosolvent Enhanced Lignocellulosic Fractionation Process. *ACS Sustainable Chemistry & Engineering* **2018**, *6* (7), 8711-8718.
48. Balakshin, M.; Capanema, E., On the Quantification of Lignin Hydroxyl Groups With ³¹P and ¹³C NMR Spectroscopy. *J. Wood Chem. Technol.* **2015**, *35* (3), 220-237.

49. Bian, H.; Chen, L.; Gleisner, R.; Dai, H.; Zhu, J. Y., Producing wood-based nanomaterials by rapid fractionation of wood at 80 °C using a recyclable acid hydrotrope. *Green Chemistry* **2017**, *19* (14), 3370-3379.
50. Wang, Y.-Y.; Li, M.; Wyman, C. E.; Cai, C. M.; Ragauskas, A. J., Fast Fractionation of Technical Lignins by Organic Cosolvents. *ACS Sustainable Chemistry & Engineering* **2018**, *6* (5), 6064-6072.
51. Cao, J.; Xiao, G.; Xu, X.; Shen, D.; Jin, B., Study on carbonization of lignin by TG-FTIR and high-temperature carbonization reactor. *Fuel Process. Technol.* **2013**, *106*, 41-47.
52. Kajihara, M.; Aoki, D.; Matsushita, Y.; Fukushima, K., Synthesis and characterization of lignin-based cationic dye-flocculant. *J. Appl. Polym. Sci.* **2018**, *135* (32), 46611.
53. Prola, L. D. T.; Machado, F. M.; Bergmann, C. P.; de Souza, F. E.; Gally, C. R.; Lima, E. C.; Adebayo, M. A.; Dias, S. L. P.; Calvete, T., Adsorption of Direct Blue 53 dye from aqueous solutions by multi-walled carbon nanotubes and activated carbon. *Journal of Environmental Management* **2013**, *130*, 166-175.
54. Li, X.; He, Y.; Sui, H.; He, L., One-Step Fabrication of Dual Responsive Lignin Coated Fe₃ O₄ Nanoparticles for Efficient Removal of Cationic and Anionic Dyes. *Nanomaterials (Basel)* **2018**, *8* (3), 162.
55. Olivo-Alanis, D.; Garcia-Reyes, R. B.; Alvarez, L. H.; Garcia-Gonzalez, A., Mechanism of anaerobic bio-reduction of azo dye assisted with lawson-immobilized activated carbon. *J. Hazard. Mater.* **2018**, *347*, 423-430.
56. Vahidhabanu, S.; Adeogun, A. I.; Babu, B. R., Biopolymer-Grafted, Magnetically Tuned Halloysite Nanotubes as Efficient and Recyclable Spongelike Adsorbents for Anionic Azo Dye Removal. *ACS Omega* **2019**, *4* (1), 2425-2436.
57. Goscianska, J.; Pietrzak, R., Removal of tartrazine from aqueous solution by carbon nanotubes decorated with silver nanoparticles. *Catal. Today* **2015**, *249*, 259-264.
58. Asfaram, A.; Ghaedi, M.; Dashtian, K.; Ghezelbash, G. R., Preparation and Characterization of Mn_{0.4}Zn_{0.6}Fe₂O₄ Nanoparticles Supported on Dead Cells of *Yarrowia lipolytica* as a Novel and Efficient Adsorbent/Biosorbent Composite for the Removal of Azo Food Dyes: Central Composite Design Optimization Study. *ACS Sustainable Chemistry & Engineering* **2018**, *6* (4), 4549-4563.
59. Mahmoodi, N. M.; Roudaki, M. S. M. A.; Didehban, K.; Saeb, M. R., Ethylenediamine/glutaraldehyde-modified starch: A bioplatfrom for removal of anionic dyes from wastewater. *Korean J. Chem. Eng.* **2019**, *36* (9), 1421-1431.
60. Dotto, G. L.; Vieira, M. L. G.; Pinto, L. A. A., Kinetics and Mechanism of Tartrazine Adsorption onto Chitin and Chitosan. *Industrial & Engineering Chemistry Research* **2012**, *51* (19), 6862-6868.
61. Oladipo, A. A.; Gazi, M.; Yilmaz, E., Single and binary adsorption of azo and anthraquinone dyes by chitosan-based hydrogel: Selectivity factor and Box-Behnken process design. *Chem. Eng. Res. Des.* **2015**, *104*, 264-279.

62. Konicki, W.; Cendrowski, K.; Chen, X.; Mijowska, E., Application of hollow mesoporous carbon nanospheres as an high effective adsorbent for the fast removal of acid dyes from aqueous solutions. *Chem. Eng. J.* **2013**, *228*, 824-833.
63. Zhao, J.; Lu, Z.; He, X.; Zhang, X.; Li, Q.; Xia, T.; Zhang, W.; Lu, C., Fabrication and Characterization of Highly Porous Fe(OH)₃@Cellulose Hybrid Fibers for Effective Removal of Congo Red from Contaminated Water. *ACS Sustainable Chemistry & Engineering* **2017**, *5* (9), 7723-7732.
64. Wang, Y.; Zhu, L.; Wang, X.; Zheng, W.; Hao, C.; Jiang, C.; Wu, J., Synthesis of aminated calcium lignosulfonate and its adsorption properties for azo dyes. *Journal of Industrial and Engineering Chemistry* **2018**, *61*, 321-330.
65. Wang, X.; Jiang, C.; Hou, B.; Wang, Y.; Hao, C.; Wu, J., Carbon composite lignin-based adsorbents for the adsorption of dyes. *Chemosphere* **2018**, *206*, 587-596.
66. Meng, X.; Crestini, C.; Ben, H.; Hao, N.; Pu, Y.; Ragauskas, A. J.; Argyropoulos, D. S., Determination of hydroxyl groups in biorefinery resources via quantitative ³¹P NMR spectroscopy. *Nature Protocols* **2019**, *14* (9), 2627-2647.

For Table of Contents Only:

